



HAL
open science

Characterization of GDP-mannose Dehydrogenase from the Brown Alga *Ectocarpus siliculosus* Providing the Precursor for the Alginate Polymer

Raimund Tenhaken, Elena Voglas, J. Mark Cock, Volker Neu, Christian G Huber

► **To cite this version:**

Raimund Tenhaken, Elena Voglas, J. Mark Cock, Volker Neu, Christian G Huber. Characterization of GDP-mannose Dehydrogenase from the Brown Alga *Ectocarpus siliculosus* Providing the Precursor for the Alginate Polymer. *Journal of Biological Chemistry*, 2011, 286 (19), pp.16707 - 16715. 10.1074/jbc.m111.230979 . hal-01925539

HAL Id: hal-01925539

<https://univ-rennes.hal.science/hal-01925539>

Submitted on 16 Nov 2018

HAL is a multi-disciplinary open access archive for the deposit and dissemination of scientific research documents, whether they are published or not. The documents may come from teaching and research institutions in France or abroad, or from public or private research centers.

L'archive ouverte pluridisciplinaire **HAL**, est destinée au dépôt et à la diffusion de documents scientifiques de niveau recherche, publiés ou non, émanant des établissements d'enseignement et de recherche français ou étrangers, des laboratoires publics ou privés.

Characterization of GDP-mannose Dehydrogenase from the Brown Alga *Ectocarpus siliculosus* Providing the Precursor for the Alginate Polymer^[S]

Received for publication, February 15, 2011, and in revised form, March 22, 2011. Published, JBC Papers in Press, March 24, 2011, DOI 10.1074/jbc.M111.230979

Raimund Tenhaken^{†1}, Elena Voglas[‡], J. Mark Cock[§], Volker Neu[¶], and Christian G. Huber[¶]

From the [†]Department of Cell Biology, Division of Plant Physiology, University of Salzburg, 5020 Salzburg, Austria, the [§]Algal Genetics Group, Marine Plants and Biomolecules Station, F-29682 Roscoff, France, and the [¶]Department of Molecular Biology, Division of Chemistry and Bioanalytics, University of Salzburg, 5020 Salzburg, Austria

Alginate is a major cell wall polymer of brown algae. The precursor for the polymer is GDP-mannuronic acid, which is believed to be derived from a four-electron oxidation of GDP-mannose through the enzyme GDP-mannose dehydrogenase (GMD). So far no eukaryotic GMD has been biochemically characterized. We have identified a candidate gene in the *Ectocarpus siliculosus* genome and expressed it as a recombinant protein in *Escherichia coli*. The GMD from *Ectocarpus* differs strongly from related enzymes in bacteria and is as distant to the bacterial proteins as it is to the group of UDP-glucose dehydrogenases. It lacks the C-terminal ~120 amino acid domain present in bacterial GMDs, which is believed to be involved in catalysis. The GMD from brown algae is highly active at alkaline pH and contains a catalytic Cys residue, sensitive to heavy metals. The product GDP-mannuronic acid was analyzed by HPLC and mass spectroscopy. The K_m for GDP-mannose was 95 μM , and 86 μM for NAD^+ . No substrate other than GDP-mannose was oxidized by the enzyme. In gel filtration experiments the enzyme behaved as a dimer. The *Ectocarpus* GMD is stimulated by salts even at low molar concentrations as a possible adaptation to marine life. It is rapidly inactivated at temperatures above 30 °C.

Ectocarpus siliculosus is a marine photoautotrophic brown alga (Phaeophyceae) which, together with oomycetes and diatoms, belongs to the phylum Stramenopiles. This phylum originated approximately 1 billion years ago as a result of a secondary endosymbiotic event, in which a unicellular red alga was captured by an ancestral protist (1).

The cell walls of brown algae differ from those of land plants (for a recent review, see Ref. 2). Along with a minor amount of cellulose, the major cell wall polysaccharide of brown algae is alginate, which accounts for up to 45% of the dry weight (3). The function of alginate in the cell walls of brown algae is similar to the function of cellulose in the cell walls of land plants. Alginate is an unbranched polysaccharide initially synthesized as a β -1,4-D-mannuronic acid chain (M-alginate). The polymer is later modified by C-5 epimerases, which convert single residues

or larger blocks of the polymer from D-mannuronic acid into L-guluronic acid (G-alginate). The M- and G-blocks in alginate vary during algae development. G-block-rich alginate will form a high strength gel in the presence of divalent cations (e.g. Ca^{2+}). M-blocks are more flexible and are preferentially found in blades exposed to wave action (3). The genes for C-5 epimerase converting M- into G-alginate have been identified in the brown alga *Laminaria digitata* (4). *L. digitata* possesses six different genes for such epimerases, which all show homology to characterized alginate epimerases (*AlgG*) from *Pseudomonas aeruginosa*. Apart from these epimerases, no other enzyme of the alginate pathway has been characterized at the molecular level (2). Bacterial alginate has similar properties to brown algal alginate but is often additionally modified by O-acetyl groups at C2 or C3 (5).

The commercial interest in alginate is manifold. Alginates are widely used to form gels e.g. to immobilize enzymes, to thicken food, or to cover organs during transplantation as a barrier between the transplant and the host immune system (6).

The precursor of alginate for alginate-producing bacteria such as *P. aeruginosa* (7) and the brown algae *Fucus gardneri* (8) is GDP-mannuronic acid (GDP-ManA).² So far, no eukaryotic enzyme for the production of GDP-ManA has been identified and characterized biochemically. GDP-ManA is derived by a four-electron oxidation of GDP-mannose (GDP-Man). The enzyme GDP-mannose dehydrogenase (GMD; EC 1.1.1.132) catalyzes the reaction $\text{GDP-Man} + 2\text{NAD}^+ \rightarrow \text{GDP-ManA} + 2\text{NADH}$ and was first purified and characterized from *Pseudomonas* (9). The enzyme belongs to the superfamily of UDP-glucose/GDP-mannose dehydrogenases which are ubiquitously present in all organisms. In bacteria this superfamily includes enzymes that oxidize different sugars such as UDP-glucose, GDP-mannose, UDP-N-acetylglucosamine, UDP-N-acetyl-D-mannosaminuronic acid, and UDP-galactose. All known eukaryotic members of the group convert only UDP-glucose. Therefore the recently published genome of the brown algae *E. siliculosus* (10) provides an excellent tool to search for and characterize a first eukaryotic GMD.

^[S] The on-line version of this article (available at <http://www.jbc.org>) contains supplemental Figs. S1–S6.

¹ To whom correspondence should be addressed: Dept. of Cell Biology, Division of Plant Physiology, University of Salzburg, Hellbrunnerstr. 34, 5020 Salzburg, Austria. Tel.: 43-662-8044-5551; Fax: 43-662-8044-619; E-mail: raimund.tenhaken@sbg.ac.at.

² The abbreviations used are: GDP-ManA, GDP-D-mannuronic acid; CID, collision-induced dissociation; ESI, electrospray ionization; EST, expressed sequence tag; GDP-Man, GDP-D-mannose; GMD, GDP-mannose dehydrogenase; IPTG, isopropyl 1-thio- β -D-galactopyranoside; MBP, maltose-binding protein; TEV, tobacco etch virus; UGD, UDP-glucose dehydrogenase.

GMD from *E. siliculosus* as Alginate Polymer Precursor

We are studying UDP-glucose dehydrogenases from plants, which are involved in providing UDP-sugars for pectic polymers, arabinans, and xyloglucans. All of these enzymes are highly substrate-specific and convert only UDP-glucose into UDP-glucuronic acid. The genome of *E. siliculosus* contains a gene with high homology to UDP-glucose dehydrogenases, suggesting to us that the alginate precursor GDP-ManA is likely generated by a specific GMD enzyme and not by UDP-glucose dehydrogenase with broad substrate specificity. Here, we characterize a unique recombinant GMD enzyme from *Ectocarpus* at the molecular level and compare its structure and properties with bacterial enzymes.

EXPERIMENTAL PROCEDURES

Chemicals—LB medium, IPTG, and glycine were from Duchefa, Tris buffer, all nucleotide sugars, nucleotides, and inhibitors were from Sigma. Phosphate buffers salts and NAD^+ were from Carl Roth (Karlsruhe, Germany). All chemicals were analytical grade or of higher purity.

Cloning of the GMD Gene—To identify candidate genes for GDP-Man dehydrogenase we searched the *E. siliculosus* genome sequence and the GenBank EST library using the soybean UDP-glucose dehydrogenase gene as a query. The blast search revealed four significant hits (see Fig. 1), a close homolog of the UDP-glucose dehydrogenase and three distantly related sequences, considered to be candidates for GDP-Man dehydrogenases. One candidate gene for GDP-Man dehydrogenase was amplified by PCR from *E. siliculosus* cDNA. RNA was reverse-transcribed using the RevertAid enzyme (Fermentas, Thermo Scientific). The following primers (forward, atggatcatgccaggaaaggagaacg; reverse, tgaagcttcaccgagctcaactgt) were used to amplify the GMD gene with Phusion proofreading polymerase. The PCR program was as follows: 98 °C 30s; 25× (98 °C 5s; 56 °C 15s; 72 °C 20s); 72 °C 2 min. The PCR product was cleaved with BamHI and HindIII and cloned into the *Escherichia coli* expression vector pMBP-Parallel1 (11), which was modified to allow fusions with a His₆-tagged maltose-binding protein (MBP) to be generated. The fusion proteins encoded by this construct possessed a TEV protease cleavage site between the MBP and the EsGMD1 protein. The sequence of the fusion construct was verified by DNA sequencing (Eurofins).

Expression in *E. coli* and Protein Purification—The expression vector was transformed into T7-Express *E. coli* cells (NEB Biolabs). For the production of recombinant proteins, 400 ml of *E. coli* culture in a 2-liter flask was grown to an $A_{600\text{ nm}}$ of ~0.4 at 37 °C, cooled to 25 °C, and induced with 0.5 mM IPTG for 16 h. Cells were then collected by centrifugation and stored frozen. The protein was purified with a Protrino 1000 column (Machery-Nagel) following the manufacturer's protocol, except that it was necessary to supplement all buffers with 200 μM NAD^+ to maintain the enzyme in an active form. All purification procedures were carried out on ice. The eluate of the Protrino column was applied to a small gel filtration column (PD10; GE Healthcare) to bring the enzyme into a suitable storage buffer (20 mM Tris-Cl, pH 8, 50 mM KCl, 200 μM NAD^+ , 1 mM DTT, 1 mM EDTA, 20% glycerol). The enzyme was snap frozen in aliquots in liquid nitrogen and stored at -80 °C. Aliquots retain their activity over several months when stored at -80 °C.

Enzyme Assay—The routine enzyme assay is based on the increase of NADH measured as an increase in $A_{340\text{ nm}}$. This can be performed easily in microcuvettes as well as in microtiter plates. The standard assay buffer consisted of 50 mM Tris-glycine buffer, pH 8.75, 1 mM NAD^+ , 0.5 mM GDP-Man, to which the EsGMD1 enzyme (typically 20–30 μg) was added. We compared the kinetic parameters of the MBP-EsGMD1 fusion protein with the TEV-cleaved EsGMD1 alone but did not find any differences in the catalytic properties. Therefore, the MBP fusion protein was used routinely in the experiments.

Cleavage at the TEV Site—One mg of EsGMD1 was incubated in 50 mM NaCl, 1 mM EDTA, 2 mM DTT, 50 mM Tris-Cl, pH 7.5, with 75 μg recombinant TEV protease (a kind gift from Prof. Hans Brandstetter, Department of Structural Biology, University of Salzburg) at 10 °C for 5 h. The activity of the GMD remains constant over this period. The TEV protease releases the pure EsGMD1 in an active form. The protein was applied to a Superose 12 column (GE Healthcare) to determine the size of the protein by gel permeation chromatography. A 50 mM Tris-Cl, pH 8, buffer with 150 mM NaCl was used at a flow rate of 0.4 ml min^{-1} to separate proteins by size. Fractions of 0.33 ml were analyzed for enzymatic activity. Standard proteins of known molecular mass were run under identical conditions.

HPLC Analysis of Products of the Enzyme Assay—The standard EsGMD1 enzyme assay was stopped by adding 1 volume of sodium phosphate buffer (100 mM, pH 3). The assay was cleared by a 5-min centrifugation and applied to a Partisil 10 SAX column (3 × 125 mm). Buffer A was 10 mM sodium phosphate, pH 3. Buffer B was 750 mM sodium phosphate, pH 3.7. The following method was used for separation: flow rate 0.75 ml min^{-1} ; $t_{0\text{ min}}$ 3% B; $t_{25\text{ min}}$ 40% B; $t_{33\text{ min}}$ 75% B; $t_{35\text{ min}}$ 75% B; $t_{36\text{ min}}$ 3% B. A UV spectrum (240–300 nm) was recorded with a photodiode array (Dionex Ultimate 3000) and analyzed with the Chromeleon software.

Direct Infusion Experiments and MS Parameters—To prepare metabolites for ESI-Orbitrap-MS measurements a standard assay was incubated for 2 h to allow the formation of sufficient GDP-ManA. The assay (1 ml) was applied to a 100-mg EnviCarb solid phase extraction column (Supelco) that had been activated before use by a short wash with 80% acetonitrile/0.1% TFA and equilibrated with 3 ml of water. The column was washed with 2 ml of H₂O to wash out buffer salts. The bound nucleotide sugars were eluted with 2 ml of 50% acetonitrile and concentrated 5-fold in an Eppendorf vacuum centrifugator.

For direct infusion experiments, an LTQ-Orbitrap XL mass spectrometer (Thermo Scientific) equipped with an Ion Max ESI source was fine-tuned in negative ionization mode, using 0.5 $\mu\text{g}/\text{ml}$ GDP-Man at $m/z = 604.07$ as the tuning mass. Finally, the solid-phase extraction column purified assay was diluted 1/1 with acetonitrile containing 0.1% formic acid as additive. Acetonitrile (Optigrade for LC/MS) was purchased from Promochem (Wesel, Germany) and formic acid (98–100%, puriss.) was from Riedel-de Haën (Hannover, Germany). The solution was directly infused using a syringe pump with a flow rate of 5.0 $\mu\text{l} \cdot \text{min}^{-1}$. The mass spectrometric parameters were as follows: mass analyzer, FTMS; resolution, 30,000; scan rate, normal; maximal injection time, 10 ms; ion polarity, negative. The optimized ESI source parameters were: source volt-

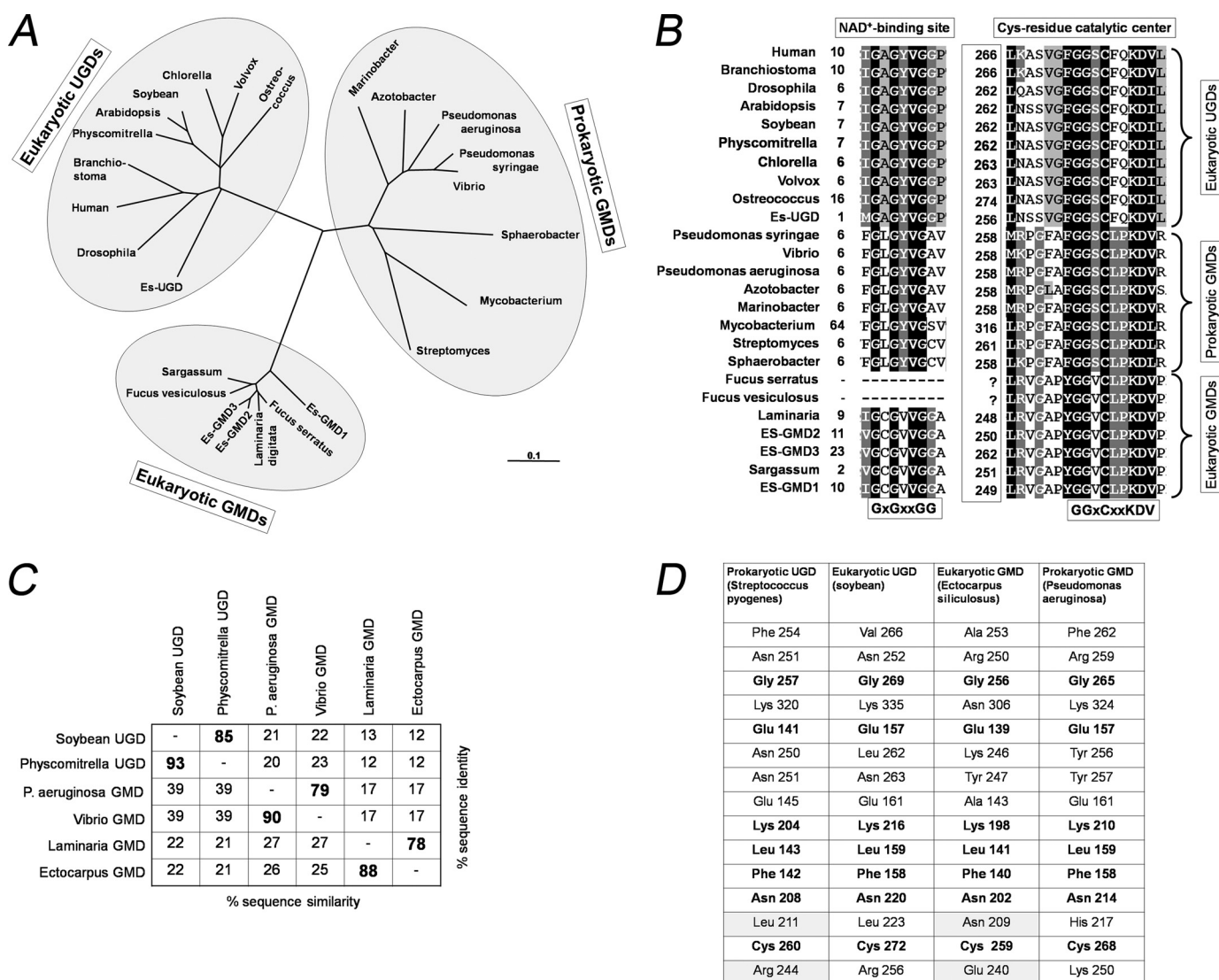


FIGURE 1. Unrooted phylogenetic tree of selected nucleotide sugar dehydrogenases and structural motifs. A, amino acid sequences were aligned with ClustalX, and a bootstrapped neighbor joining tree was used to calculate the distance between the sequences. **UGDs:** soybean, U53418; *Arabidopsis*, At3g29360; *Ectocarpus*, Esi0101_0043; human, NP_003350; *Drosophila*, AAC97125; *Physcomitrella patens*, XP_001761641; *Chlorella variabilis*, FEN57705; *Volvox carter*, XP_002945908; *Ostreococcus tauri*, XP_003082645; *Branchiostoma floridae*, XP_002606188. **Eukaryotic GMDs:** *Ectocarpus* GMD1, Esi0164_0053; *Ectocarpus* GMD2, Esi0051_0113; *Ectocarpus* GMD3, Esi0051_0092; *Sargassum binderi*, ESTs DV668856 + DV669914; *Fucus serratus*, ESTs GH701299 + GH69914; *Laminaria digitata*, ESTs CN466747 + CN468196 + CN466724; *Fucus vesiculosus*, GH704760. **Prokaryotic GMDs:** *P. aeruginosa*, P11759; *Pseudomonas syringae*, P59793; *Azotobacter*, P51585; *Mycobacterium smegmatis*, YP_890183; *Vibrio sp.*, ABP49558; *Marinobacter algicola*, ZP_01893737; *Sphaerobacter thermophilus*, YP_003319392; *Streptomyces violaceusniger*, ZP_07604805. B, from the sequences shown in the tree in A the NAD⁺ binding site close to the N terminus and the region around the catalytic Cys residue are shown. Note that the two sequence motifs are highly conserved in all three groups of proteins but still show group specific differences. C, two representative sequences from each subgroup were compared for sequence identity and sequence similarity. The identity among different subgroups is low ~20%. D, ligand-binding amino acid residues from different UGDs and GMDs are compared.

age, 2.5 kV; capillary voltage, -35 V; capillary temperature, 280 °C; sheath gas flow, 15 arb. units; aux gas flow, 5 arb. units; tube lens, -89.32 V. The molecular formulas and mass deviations were calculated by using XCalibur software version 2.0.7 (Thermo Fisher Scientific).

RESULTS

Phylogenetic Analysis of Ectocarpus GMD—The recent sequencing of the alginate producing brown alga *E. siliculosus* (10) allowed us to search for nucleotide sugar dehydrogenases, which provide the alginate precursor GDP-ManA. So far in eukaryotes, only one type of nucleotide sugar dehydrogenase, UDP-glucose dehydrogenase (UGD), has been identified and

characterized biochemically. UGDs are ubiquitously present in animals, fungi, and plants. Indeed, *E. siliculosus* contains a single gene, which clusters with UGD sequences from plants and animals (Fig. 1A) but in addition has three further genes that are clearly distinct from the UGD and are thus candidate genes for a GMD. A multiple alignment of bacterial GMDs, the *E. siliculosus* candidate GMD, related candidate genes from brown algae assembled from the GenBank EST database and a selection of UGDs is shown as a tree in Fig. 1A and as full alignment in supplemental Fig. S1. As expected, all UGDs cluster in one branch of the unrooted tree, as do the bacterial GMDs. However, the GMDs from *E. siliculosus* and four other brown algae fall into a distinct third branch almost as distant from the bac-

GMD from *E. siliculosus* as Alginate Polymer Precursor

terial GMDs as from the UGDs. Because the three *E. siliculosus* GMD sequences are highly similar to each other, we decided to focus on one of the genes *EsGMD1*, which is encoded by *Esi0164_0053* and for which there are several EST sequences (supplemental Fig. S2).

Structural Motif Conservation—The full alignment of all sequences from the tree in Fig. 1A is shown in supplemental Fig. S1. The protein sequences of the GMD from *P. aeruginosa* and *EsGMD1* from *E. siliculosus* are broadly collinear with the exception of a 19-amino acid gap in the *EsGMD1* sequence. However, *EsGMD1* is considerably shorter than the bacterial GMDs and lacks the C-terminal extensions of these proteins. All three *E. siliculosus* GMDs as well as the GMDs from *Laminaria*, *Fucus*, and *Sargassum*, lack the C-terminal extension typically found in all bacterial GMDs (supplemental Fig. S1). The sequence of *EsGMD1* was corroborated by finding eight overlapping EST clones spanning the full-length coding sequence of the gene (supplemental Fig. S2). Therefore, we consider the *EsGMD1* sequence as a full-length open reading frame.

Two signatures of nucleotide sugar dehydrogenases, the NAD^+ binding site at the N terminus and the catalytic center around a highly conserved cysteine residue are shown in Fig. 1B for all the proteins of the phylogenetic tree from Fig. 1A. The three clusters, eukaryotic UGDs, eukaryotic GMDs, and prokaryotic GMDs each have distinct sequence motifs around the conserved NAD^+ binding site as well around the catalytic site, which can be considered as typical for each of the subgroups (Fig. 1B). The overall sequence identity/similarity between two bacterial GMDs, two brown algae GMDs, and two plant UGDs is shown in Fig. 1C. The identity between bacterial and brown algae GMDs is $\sim 17\%$ ($\sim 26\%$ similarity).

The GMD protein from *P. aeruginosa* (12) and the UGD protein from *S. pyogenes* (13) were recently crystallized. The structure prediction tool Phyre indicates a similar overall structure of the *Ectocarpus* GMD compared with the crystallized UGD and GMD proteins. Thus substrate interacting amino acid residues were identified. By combining the information from the publications by Snook *et al.* (12) and Campbell *et al.* (13) along with our sequence alignment we were able to predict putative substrate interacting residues of the *E. siliculosus* GMD (Fig. 1D). Substrate-interacting amino acid residues of the bacterial GMD (Protein Data Bank ID code 1MUU) are shown in supplemental Fig. S3. Most of the substrate binding residues are identical in UGD and GMD sequences, indicating a common evolutionary origin. Notably, the Arg^{244} from *S. pyogenes* UGD which makes hydrogen bonds to the OH groups at C2 and C3 from the glucose of UDP-glucose is replaced by a Glu residue in *EsGMD1*. This could be a structural requirement for binding GDP-Man, which differs in the steric orientation of the C2-OH group from mannose relative to glucose.

Expression and Purification of Recombinant GMD—To characterize and confirm the GMD function of *EsGMD1*, we expressed the enzyme as a recombinant fusion protein with the MBP. Attempts to obtain *EsGMD1* with a His tag alone were unsuccessful and resulted in inclusion body formation under a variety of conditions (5–500 μM IPTG as inducer; 37 $^{\circ}\text{C}$ –15 $^{\circ}\text{C}$ for induction; different *E. coli* strains). The engineered

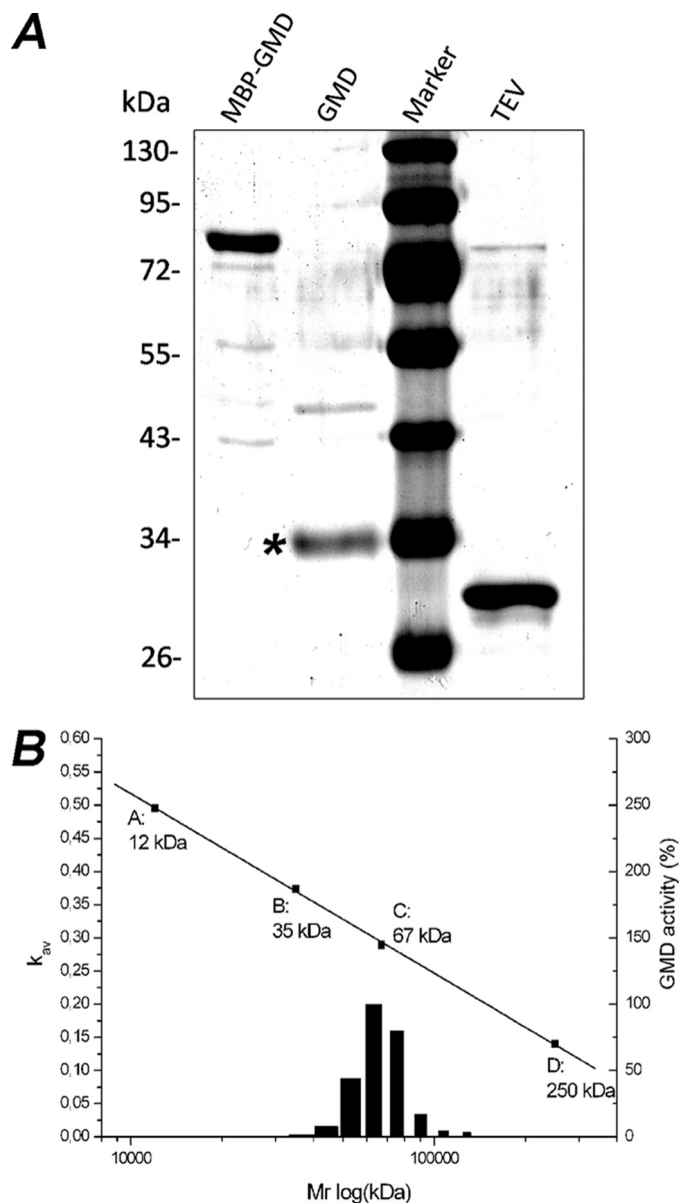


FIGURE 2. A, SDS-PAGE of recombinant MBP-GMD from *Ectocarpus*. First lane, recombinant *EsGMD1* as MBP fusion protein. Second lane, *EsGMD1* after cleavage and removal of the MBP (marked with an asterisk). Third lane, molecular mass markers. Fourth lane, recombinant TEV protease used to cleave off the MBP. B, size exclusion chromatography of *EsGMD1* (without MBP). 200- μl samples were separated on a Superose 12 column, and fractions of 0.33 ml were collected and analyzed for activity (black bars). The column was calibrated with standard proteins of known molecular mass (A, cytochrome c; B, β -lactoglobulin; C, BSA; D, catalase). The *EsGMD1* protein (34 kDa) elutes at approximately 68 kDa, suggesting that it runs as a dimer.

fusion protein contains a TEV protease cleaving site in front of the GMD protein which allows it to be cleaved from the MBP fusion partner (Fig. 2). On a 10% SDS-PAGE the purified *EsGMD1* ran as a 34-kDa protein consistent with the predicted theoretical mass of 34.528 kDa.

The *Pseudomonas* GMD is believed to be active as a hexamer (9, 14). We therefore separated *EsGMD1* protein on a Superose 12 FPLC size exclusion column. GMD activity plotted against the molecular mass is shown in Fig. 2B, revealing a maximum between 65 and 70 kDa. This fits very well with the hypothesis that *EsGMD1* forms a dimeric complex.

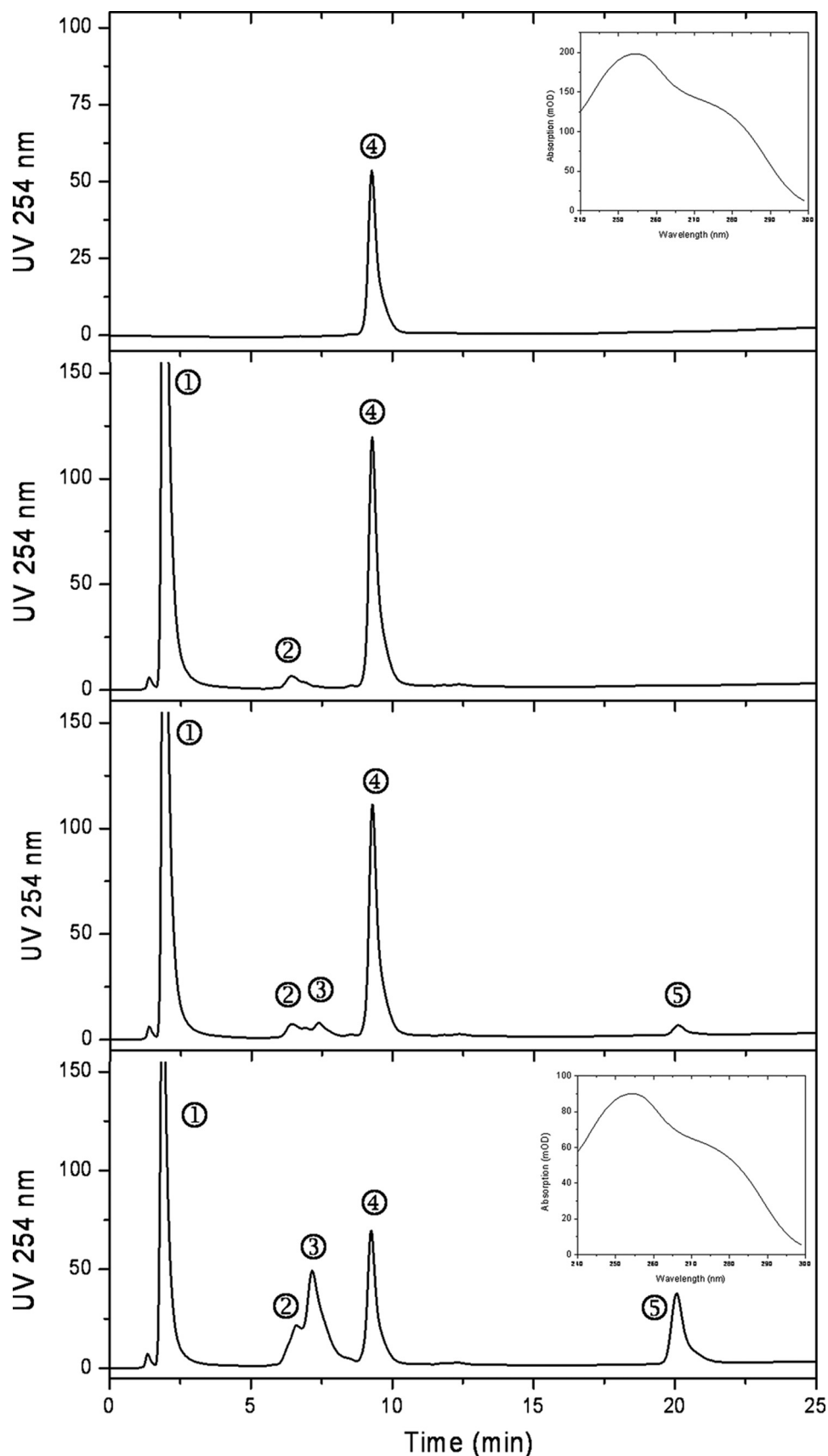
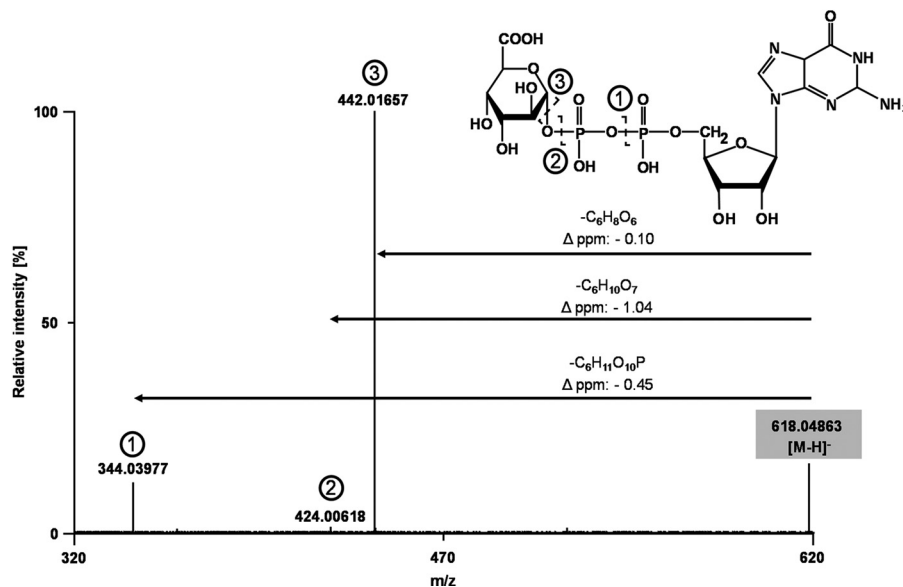
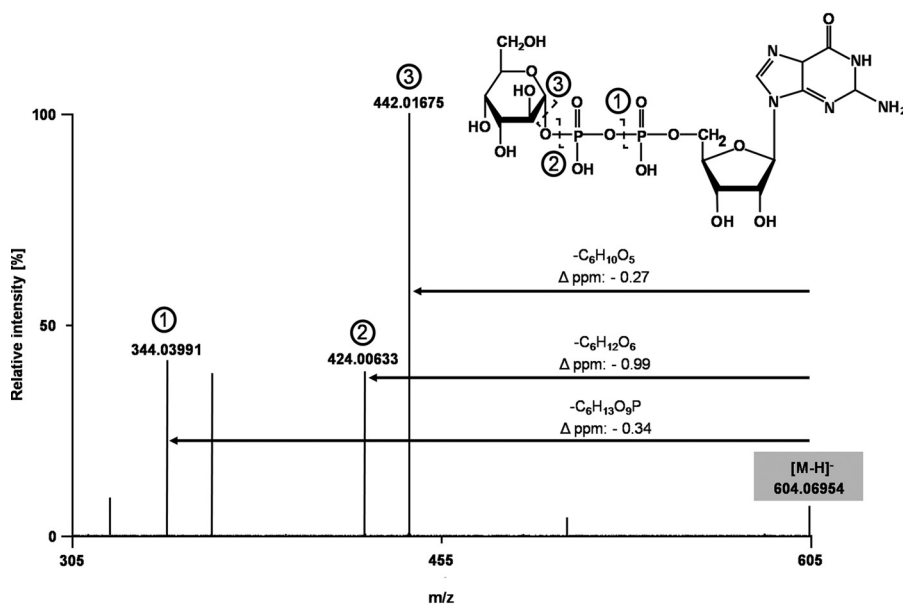
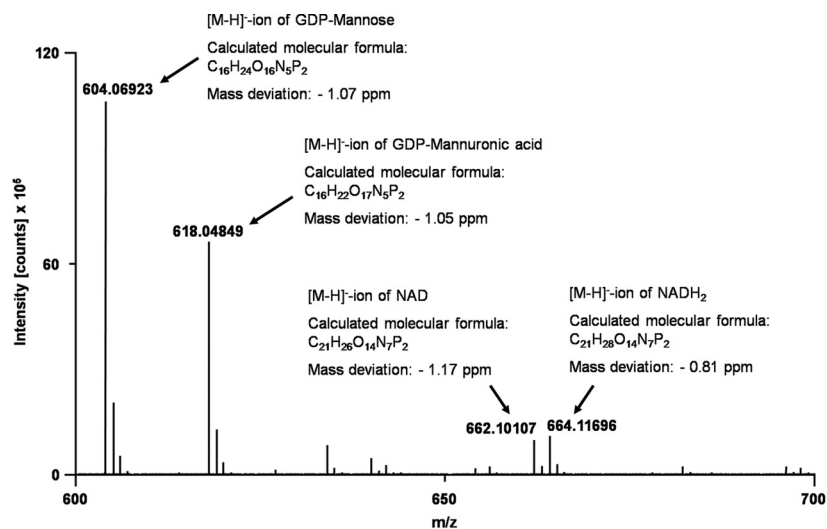


FIGURE 3. **HPLC chromatography of enzyme assays.** The *top trace* shows the separation of the substrate GDP-Man and a UV spectrum as the *inset*. The *second trace* shows an enzyme assay, from which the EsGMD1 enzyme was omitted. The *two bottom traces* show a full enzyme assay after 5 and 60 min, respectively. The UV spectrum of the product GDP-ManA (5) is shown in the *lower inset* (1). NAD⁺; 2, unknown impurity from NAD⁺; 3, NADH; 4, GDP-Man; 5, GDP-ManA.

GMD from *E. siliculosus* as Alginate Polymer Precursor



Enzyme Assay and Product Confirmation—The enzymatic activity of EsGMD1 was confirmed by HPLC and ESI-MS analysis. A series of HPLC chromatograms is shown in Fig. 3. The commercial substrate GDP-Man (4) was separated in the *uppermost trace*. The *inset* shows a typical guanosine UV spectrum. The *second trace* shows a control assay without the recombinant enzyme added. Compound 1 is NAD⁺, 2 is an unknown impurity in the NAD⁺. The *two bottom chromatograms* show two time points of a typical GMD assay after 5 and 60 min, respectively. Compound 3 is NADH, a product of the reaction. The novel compound 5 is GDP-ManA and has the same UV spectrum as GDP-Man. A comparison of the peak areas of the substrate GDP-Man (4) and the product GDP-ManA (5) for several assays shows a constant peak area sum of both metabolites indicating the direct conversion of 4 into 5. To verify the identity of the GMD-ManA we purified the nucleotide sugars from an enzyme assay by solid phase extraction on an EnviCarb column. The salt-free extract was then analyzed by ESI-Orbitrap-MS (Fig. 4). The signals of GDP-Man, GDP-ManA, NAD⁺, and NADH were readily identified with high abundance and mass accuracies in the sub-ppm range. GDP-ManA shows the predicted mass increase of 14 mass units resulting from the oxidation of the alcoholic C6 group into a carboxylic acid group. CID fragmentation of GDP-Man and GDP-ManA results in the loss of Man/ManA either with or without the oxygen atom at C1 of the sugar (Fig. 4, *middle* and *bottom*).

Biochemical Characterization of the Enzyme—We next proceeded with a detailed biochemical characterization of EsGMD1. The enzyme has an alkaline pH optimum around 8.75–9 and is inactive below pH 7 (supplemental Fig. S4). EsGMD1 is quite sensitive to certain buffers, such as diethanolamine, which totally inhibits all enzyme activity. All further assays were performed in Tris-glycine buffer, pH 8.75.

EsGMD1 is temperature-sensitive. The activity steadily increases from 0 °C to 30 °C but strongly declines above 30 °C. An incubation period of 15 min at 45 °C fully inactivates EsGMD1.

The kinetic parameters of EsGMD1 follow typical Michaelis-Menten kinetics. Using the minimum square deviation method to fit the hyperbolic data, we obtained a K_m of 95 μM for the substrate GDP-Man and a K_m of 86 μM for the cofactor NAD⁺ (supplemental Fig. S5). The k_{cat} value of the purified recombinant GMD is $0.21 \cdot \text{s}^{-1}$. The specific activity of recombinant EsGMD1 is 3.3 nanokatals mg^{-1} protein. *E. siliculosus* is a marine alga living in a salty environment. This prompted us to analyze the effect of mono- and divalent salts on GMD activity. All salts led to an increase in enzymatic activity. The optimum is approximately 500 mM for Na₂SO₄ and NaCl and slightly lower for KCl. Even the presence of 1.5 M salts increases the

TABLE 1
Substrate specificity of *Ectocarpus* EsGMD1

| Substrates | Enzyme activity |
|----------------------------------|-----------------|
| | % of control |
| GDP-mannose (Control) | 100 ± 0.7 |
| GDP-glucose | 0 |
| UDP-glucose | 0 |
| UDP- <i>N</i> -acetylglucosamine | 0 |
| UDP-galactose | 0 |

TABLE 2
Inhibitors of EsGMD1

| Treatment | Enzyme activity |
|---|-----------------|
| | % of control |
| Control | 100 ± 0.7 |
| Nucleotides | |
| ATP (1 mM) | 97 ± 0.8 |
| UTP (1 mM) | 96 ± 0.5 |
| UDP (1 mM) | 102 ± 0.6 |
| UMP (1 mM) | 101 ± 0.8 |
| Chelator, metals, and modifying reagents | |
| EDTA (1 mM) | 105 ± 0.9 |
| CoCl ₂ (1 mM) | 44.8 ± 0.6 |
| CuSO ₄ (1 mM) | 0 ± 0.01 |
| FeCl ₃ (1 mM) | 49 ± 0.5 |
| FeSO ₄ (1 mM) | 77.4 ± 0.5 |
| pCMB (1 μM) | 99 ± 0.7 |
| pCMB (5 μM) | 87.9 ± 0.6 |
| pCMB (10 μM) | 20.6 ± 0.2 |
| pCMB (25 μM) | 0.8 ± 0.04 |

GMD activity compared with the 50 mM buffer alone (supplemental Fig. S6).

The substrate specificity of EsGMD1 was tested with several other nucleotide sugars, but none except GDP-Man is converted by the enzyme (Table 1). The data suggest that EsGMD1 is highly specific for the production of the alginate precursor GDP-ManA. The cofactor NAD⁺ cannot be replaced by NADP⁺, addition of the latter instead of NAD⁺ resulted in zero activity.

Some potential inhibitors of GMD were tested, and the data are summarized in Table 2. NADH is a weak inhibitor of the reaction. The decrease in enzyme activity observed after longer incubation times cannot be fully explained by the accumulation of NADH. Presumably, the product GDP-ManA is another inhibitor of the reaction. We did not determine the K_i for GDP-ManA because to our knowledge this compound is not commercially available. The catalytic cysteine is sensitive to heavy metals. In particular, copper ions and the organic mercury compound *p*-chloromercuribenzoate totally inhibit GMD at micromolar concentrations. In contrast, EDTA prevents binding of heavy metals to the Cys residue and therefore slightly increases the enzymatic activity by chelating residual heavy metals present in the buffers etc.

FIGURE 4. *Top*, high resolution full-scan mass spectrum of the solid-phase extraction column-purified assay mixture in a mass range of $m/z = 600\text{--}700$, applying negative ionization mode. *Middle*, high resolution centroid CID fragmentation spectrum of GDP-Man in a mass range of $m/z = 305\text{--}605$, applying a relative CID fragmentation energy of 25%. The precursor mass of the GDP-Man is highlighted in gray. The dashed lines in the structural formula indicate heterolytic cleavage sites due to CID fragmentation. *Bottom*, high resolution centroid CID fragmentation spectrum of GDP-ManA in a mass range of $m/z = 320\text{--}620$, applying a relative CID fragmentation energy of 19%. The precursor mass of the GDP-ManA is highlighted in gray. The dashed lines in the structural formula indicate heterolytic cleavage sites due to CID fragmentation. Molecular formulas of neutral losses and corresponding mass deviations were calculated using the XCalibur software version 2.0.7.

DISCUSSION

Properties of EsGMD1—Here we characterize the first GMD from a eukaryotic organism, the brown alga *E. siliculosus*. Previously, only the GMD from the prokaryote *P. aeruginosa* has been partially analyzed biochemically (9). Both enzymes catalyze the same reaction, the conversion of GDP-Man into GDP-ManA, but they differ widely in their biochemical properties. The K_m of EsGMD1 is roughly 5-fold higher than the reported K_m for GDP-Man of the bacterial enzyme. This difference can possibly be explained by the different roles of alginate in bacteria and algae. *E. siliculosus* does not need GDP-Man only for alginate biosynthesis, but also for the synthesis of fucan polymers destined for the cell wall. In flowering plants, GDP-Man is also an important precursor for ascorbic acid biosynthesis (15). This use of GDP-Man in several pathways in brown algae, which are all of major quantitative importance, may explain the higher K_m of the EsGMD1 to maintain the supply of GDP-Man for the other pathways. The V_{max} of EsGMD1 is ~ 3 -fold lower than that reported for the *Pseudomonas* enzyme (9).

EsGMD1 is sensitive to higher temperatures and was rapidly inactivated at 35 °C, whereas the bacterial enzyme has a temperature optimum at 50 °C. This suggests there might be unique structural features of the bacterial enzymes that impart greater enzyme stability.

EsGMD1 is a member of a small group of NAD⁺-dependent four-electron transfer dehydrogenases all of which contain a conserved catalytic Cys residue. This residue is believed to be involved in the formation of a thiohemiacetal intermediate with the substrate GDP-Man after the first two-electron oxidation step, which has also been observed in the sister enzyme UGD (13, 16). The alkaline pH optimum for EsGMD1 is approximately pH 8.5- and thus near to the pK_a -value of the Cys residue. Similar pH optima were observed for UGDs from plants (17, 18). For the *Pseudomonas* GMD Roychoudhury *et al.* (9) report a significantly lower and very sharp pH optimum of pH 7.7 which seems to be an exception for this group of enzymes.

Structural Differences between Pro- and Eukaryotic GMDs—The most striking difference between pro- and eukaryotic GMDs is the structure of the enzyme. The bacterial enzyme has been crystallized, and from this dataset several binding sites for the substrates NAD⁺ and GDP-Man were predicted (12). The structure of *Pseudomonas* GMD is composed of two large but mirrored domains that are connected by a long α -helix. The N-terminal domain (residues 1–154) shows a typical Rossmann fold and contains a complete dinucleotide binding motif with six-stranded parallel β -sheets and five α -helices. The swapped domain at the C terminus (residue 315–436), however, represents an incomplete Rossmann fold, in which the dinucleotide-binding motif is missing the third β -strand and the final α -helix (12). This second domain is completely absent in the GMDs from *E. siliculosus*, suggesting that the N-terminal Rossmann fold from the brown algal enzyme is sufficient to bind its substrates. Some speculative models for substrate binding have been proposed for the bacterial enzyme, in which the N-terminal Rossmann fold of enzyme A completes the substrate binding sites with the C-terminal incomplete Rossmann fold from enzyme B. This model was supported by the finding that GMD

genes from bacteria are all highly similar in their domain organization. Because EsGMD1 lacks the C-terminal Rossmann fold, a different mechanism of substrate binding is likely, or the N-terminal domains from two GMD-molecules completes one binding site. The latter hypothesis seems possible as EsGMD1 is active as a dimer. In this case the structure of the GMD must be very flexible, as we did not detect differences in biochemical properties between the pure EsGMD1 enzyme and the fusion protein with MBP. Discerning between these possibilities will likely require structural elucidation of the EsGMD1 enzyme.

Evolution of Ectocarpus GMD—The brown algae are phylogenetically related to another group of algae, the diatoms. Two diatom genomes have been published recently, but database homology searches produced no convincing evidence of the presence of GMD genes in diatoms. Furthermore, none of the currently more than 280 other eukaryotic genomes in GenBank, including further genomes of the *Stramenopiles* lineage, contains a GMD-like gene.

In contrast, several different bacteria have genes for GMD, which are highly similar to that characterized from *P. aeruginosa*. This could be a hint for a single evolutionary event in the *Stramenopiles* lineage, in which a bacterial GMD was taken up by early brown algae, modified drastically, and afterward maintained in different brown algae. All characteristic structural and sequence features of EsGMD1 are highly conserved between different order of brown algae like the *Ectocarpales*, *Fucales*, and *Laminariales*. *Ectocarpus* can be infected by a large genome virus EsV-1 (335-kbp genome) which has distant copy of a UGD or GMD gene in its genome (19). Such a virus could have caused a lateral gene transfer in the past, in which genes for an alginate pathway were transferred into a brown alga. A convergent evolution of the GMD in brown algae is very unlikely, as for example most of the substrate binding amino acids and the residues of the catalytic center are identical or very similar in bacterial and brown algae GMDs.

Acknowledgments—We thank Doris Wittmann and Delphine Scornet for technical help and Hans Brandstetter for valuable discussions about the structural analysis of GMD proteins and for providing the His-tagged MBP expression vector.

REFERENCES

1. Reyes-Prieto, A., Weber, A. P., and Bhattacharya, D. (2007) *Annu. Rev. Genet.* **41**, 147–168
2. Michel, G., Tonon, T., Scornet, D., Cock, J. M., and Kloareg, B. (2010) *New Phytol.* **188**, 82–97
3. Kloareg, B., and Quatrano, R. S. (1988) *Oceanogr. Marine Biol.* **26**, 259–315
4. Nyvall, P., Corre, E., Boisset, C., Barbeyron, T., Rousvoal, S., Scornet, D., Kloareg, B., and Boyen, C. (2003) *Plant Physiol.* **133**, 726–735
5. Skjåk-Braek, G., Grasdalen, H., and Larsen, B. (1986) *Carbohydr. Res.* **154**, 239–250
6. Draget, K. I., Smidsrod, O., and Skjåk-Braek, G. (2002) in *Biopolymers Polysaccharides II* (Vandamme, E. J., De Baets, S., and Steinbüchel, A., eds) pp. 215–244, Wiley-VCH, Weinheim
7. Deretic, V., Gill, J. F., and Chakrabarty, A. M. (1987) *J. Bacteriol.* **169**, 351–358
8. Lin, T. Y., and Hassid, W. Z. (1966) *J. Biol. Chem.* **241**, 5284–5297
9. Roychoudhury, S., May, T. B., Gill, J. F., Singh, S. K., Feingold, D. S., and Chakrabarty, A. M. (1989) *J. Biol. Chem.* **264**, 9380–9385

10. Cock, J. M., Sterck, L., Rouzé, P., Scornet, D., Allen, A. E., Amoutzias, G., Anthouard, V., Artiguenave, F., Aury, J. M., Badger, J. H., Beszteri, B., Billiau, K., Bonnet, E., Bothwell, J. H., Bowler, C., Boyen, C., Brownlee, C., Carrano, C. J., Charrier, B., Cho, G. Y., Coelho, S. M., Collén, J., Corre, E., Da Silva, C., Delage, L., Delaroque, N., Dittami, S. M., Doubeau, S., Elias, M., Farnham, G., Gachon, C. M., Gschloessl, B., Heesch, S., Jabbari, K., Jubin, C., Kawai, H., Kimura, K., Kloreg, B., Küpper, F. C., Lang, D., Le Bail, A., Leblanc, C., Lerouge, P., Lohr, M., Lopez, P. J., Martens, C., Maumus, F., Michel, G., Miranda-Saavedra, D., Morales, J., Moreau, H., Motomura, T., Nagasato, C., Napoli, C. A., Nelson, D. R., Nyvall-Collén, P., Peters, A. F., Pommier, C., Potin, P., Poulain, J., Quesneville, H., Read, B., Rensing, S. A., Ritter, A., Rousvoal, S., Samanta, M., Samson, G., Schroeder, D. C., Ségurens, B., Strittmatter, M., Tonon, T., Tregear, J. W., Valentin, K., von Dassow, P., Yamagishi, T., Van de Peer, Y., and Wincker, P. (2010) *Nature* **465**, 617–621
11. Sheffield, P., Garrard, S., and Derewenda, Z. (1999) *Protein Expr. Purif.* **15**, 34–39
12. Snook, C. F., Tipton, P. A., and Beamer, L. J. (2003) *Biochemistry* **42**, 4658–4668
13. Campbell, R. E., Mosimann, S. C., van De Rijn, I., Tanner, M. E., and Strynadka, N. C. (2000) *Biochemistry* **39**, 7012–7023
14. Naught, L. E., Gilbert, S., Imhoff, R., Snook, C., Beamer, L., and Tipton, P. (2002) *Biochemistry* **41**, 9637–9645
15. Conklin, P. L., Norris, S. R., Wheeler, G. L., Williams, E. H., Smirnov, N., and Last, R. L. (1999) *Proc. Natl. Acad. Sci. U.S.A.* **96**, 4198–4203
16. Ge, X., Penney, L. C., van de Rijn, I., and Tanner, M. E. (2004) *Eur. J. Biochem.* **271**, 14–22
17. Klinghammer, M., and Tenhaken, R. (2007) *J. Exp. Bot.* **58**, 3609–3621
18. Hinterberg, B., Klos, C., and Tenhaken, R. (2002) *Plant Physiol. Biochem.* **40**, 1011–1017
19. Delaroque, N., Müller, D. G., Bothe, G., Pohl, T., Knippers, R., and Boland, W. (2001) *Virology* **287**, 112–132